# Sensitivity of the upper ocean structure to atmospheric forcing

Mixed layer
Upper ocean
Heat content
Wind forcing

Couche mélangée
Océan superficiel
Contenu thermique
Forçage par le vent

Mehmet KARACA

I.T.U. Maden Fak. Genel Jeeoloji ABD, Maslak, 80626 Istanbul, Turkey.

ABSTRACT

A one-dimensional model of the upper ocean is presented. The model is based on a self-similar temperature profile (called the model-profile) and features special parameterizations of forcing functions in terms of surface heat flux and wind stress. The model-profile is combined with observational data for the Pacific Ocean to produce dynamically consistent fields of mixed-layer temperature, depth, and effective depth.

The model for the upper ocean is forced with surface heat fluxes simulated by the UCLA Atmospheric General Circulation Model (AGCM) using both climatological and observed sea-surface temperature (SST) for periods following the 1982-1983 ENSO event. Furthermore, the mixed-layer temperature is taken as the SST used in the AGCM. In this context, the model produces the wind forcing consistent with the prescribed mixed-layer temperatures and surface heat fluxes. It is found that the resulting wind forcing has significant differences with that simulated by the AGCM. A method is suggested, therefore, to evaluate surface fluxes simulated by an AGCM with a view to its eventual coupling to an Oceanic General Circulation Model (OGCM).

RÉSUMÉ

Sensibilité de la structure de l'océan superficiel au forçage atmosphérique

Un modèle unidimensionnel d'océan superficiel est présenté. Le modèle est basé sur un profil-type de température (appelé le « profil modèle ») et introduit une paramétrisation spécifique des fonctions de forçage en termes de flux de chaleur en surface et de friction due au vent. Le « profil modèle » est combiné à des données observées dans l'océan Pacifique pour produire des champs dynamiquement consistants de température, profondeur et profondeur effective de la couche mélangée.

Le modèle d'océan superficiel est forcé par des flux de chaleur simulés par le Modèle de Circulation Générale Atmosphérique (MCGA) de l'UCLA, contraint tour à tour par des Températures de Surface de la Mer (TSM) climatologiques puis observés au cours de la période suivant l'événement ENSO de 1982-83. De plus, la température de la couche mélangée choisie est la TSM utilisée dans le MCGA. Dans ce cas, le modèle produit un forçage par le vent constant avec la température de la couche mélangée imposée et avec les flux de chaleur en surface. On note que le forçage du vent résultant est significativement différent de celui simulé par le MCGA. Nous avons donc suggéré une méthode d'évaluation des flux en surface simulés par un MCGA en vue de son éventuel couplage à un Modèle de Circulation Générale Océanique (MCGO).

*Oceanologica Acta*, 1996, **19**, 1, 15-26.

## INTRODUCTION

At their interface, the atmosphere and ocean exchange heat and momentum. Also, the atmosphere supplies fresh water to the ocean, and the ocean yields moisture to the atmosphere. These exchanges are largely controlled by vertical turbulence and buoyancy fluxes in the planetary boundary layer and the oceanic mixed layer. Typical values for zonal mean heat storage in the first few hundred metres of the ocean are about five times the atmospheric values during the seasonal cycle (Oort and Von der Haar, 1976; Meehl, 1984). Heat storage in the upper ocean is subject to systematic variations due to wind-induced mixing and entrainment processes, and is strongly related to variations in Sea Surface Temperature (SST), (Oort and Von der Haar, 1976). Thus, SST depends on both air-sea interactions and the dynamics of the entire upper-ocean.

This paper has two main objectives: 1) to obtain estimates of the upper-ocean structure for the Pacific in terms of mixed-layer temperature, depth and effective depth; and 2) to present a methodology for preliminary assessment of the wind stress field produced by an Atmospheric General Circulation Model (AGCM) in anticipation of its future coupling to an Oceanic General Circulation Model (OGCM).

To achieve these objectives we use a one-dimensional model of the upper ocean based on the concepts pioneered by Kraus and Turner (1967). A preliminary version of the model is given by Karaca and Müller (1989). The model, which will be referred to as the K-M model, has two major components: a) it assumes a self-similar temperature profile called "the model-profile"; and b) it uses special parameterizations for the forcing functions in terms of surface heat flux and wind stress. The validity of the assumptions involved in the K-M model was supported by detailed comparisons between model predictions and temperature data collected by weather ships at five locations in the North Atlantic (Karaca and Müller, 1989, 1991).

The mixed-layer temperature and depth are two of the most important parameters that define the model-profile at particular locations. A procedure that consists of least-square fitting the zeroth and first-order moments of model and observed profiles allows for a physically consistent determination of mixed-layer temperature and depths. The observed profiles are obtained from the data set for the global ocean compiled by Levitus (1982). Results of our calculations are presented for the Pacific Ocean between 50° N and 50° S.

We use the K-M model to obtain an evaluation of the surface fluxes of momentum simulated by the UCLA-AGCM with prescribed SST, with a view to the eventual coupling of the AGCM to an OGCM. Current procedures for verification are based on comparisons between simulated fluxes and their counterparts derived from observational data. These procedures do not include consideration of the multiple feedbacks in the ocean-atmosphere system, nor in each of the subsystems. Our procedure uses the K-M model with mixed-layer temperatures corresponding to the SST prescribed in the AGCM boundary conditions and forcing corresponding to surface heat fluxes simulated by the AGCM to obtain the distribution of heat content in the oceanic column and the wind forcing required to produce

this distribution. The wind forcing so obtained is then compared with that simulated by the AGCM.

We begin in the next Section by presenting an outline of the K-M model, including a discussion of the model-profile and parameterizations of the model forcing functions. In Section "Temperature structure", we estimate the distributions of mixed-layer temperature, depth, and effective depth for the Pacific Ocean between 50° N and 50° S. In Section "Seasonal evaluation", we compare surface momentum fluxes from the UCLA-AGCM with a prescribed SST field corresponding to an observed climatology and the corresponding fluxes obtained using the K-M model as described above. We contrast these results with those obtained using surface heat fluxes produced by the AGCM with SSTs corresponding to the observed during the period October 1982-September 1983.

### The K-M model for the upper ocean

#### Equations of the model

One of the basic assumptions of the K-M model is that the vertical buoyancy structure of the upper ocean can be represented in terms of a self-similar, continuous temperature profile. For better agreement with observed temperature profiles, the step-wise distribution with a homogenous thermocline in the original Kraus-Turner (1967) model is replaced by another with an exponentially decaying distribution below the mixed layer. The temperature profile for the upper ocean in the K-M model is described by the analytical expression

$$
T(z, t) = \begin{cases} T_1(t) & 0 \geq z \geq -h_1 \\ T_0 + T_{10}(t)e^{D(z, t)} & -h_1 \geq z \geq -h_1 \end{cases} \quad (1)
$$

where $T_1$ is the mixed-layer temperature, $h_1$ is mixed-layer depth, $h_2$ is depth of the ocean column, $T_0$ is a reference temperature and $T_{10} = T_1 - T_0$. The exponent $D$ is given by

$$
D = (z + h_1)/h_{12}
$$

where $h_{12}$ is a scale-depth of the seasonal thermocline. The temperature $T_0$, therefore, is the asymptotic temperature of the profile. According to (1), the parameters $T_1$, $h_1$, $T_0$ and $h_{12}$ suffice to describe the profile completely. The temperature profile (1) will be referred to as the model-profile.

The scale-depth of the thermocline, $(h_{12})$, can be expressed in terms of $T_{10}$ and of $T_{20} = T_b - T_0$, where $T_b$ is the temperature at $z = -h_2$ . It follows that

$$
h_{12} = (h_2 - h_1) / \Theta \quad (2)
$$

where

$$
\Theta = \ln (T_{10} / T_{20})
$$

In this way, the model-profile is determined by the mixed-layer temperature and depth ($T_1$ and $h_1$, respectively), by the temperature ($T_b$) at a particular depth ($h_2$) in the thermocline, and by the asymptotic temperature ($T_0$). The validity of the model-profile under a wide range of ocean conditions has been well established empirically (Lemke and Manley, 1984; Lemke, 1987; Karaca and Müller, 1989).

The total buoyancy and potential energy of the ocean column are given by the zeroth and first moments of the temperature profile,

$$R_0 = \int_{-h_2}^{0} (T - T_0)dz \tag{3}$$

$$R_1 = \int_{-h_2}^{0} (T - T_0)zdz \tag{4}$$

Lengths that can be taken as representative of the thermal depth ($h_q$) and centre of gravity ($h_p$) of the ocean column are defined as

$$R_0 = T_{10}h_q \tag{5}$$

$$R_1 = R_0h_p \tag{6}$$

The following relations are satisfied if the temperature distribution is given by the model-profile (1)

$$R_0 = T_{10}h_1 + (T_{10} - T_{20})h_{12} \tag{7}$$

$$R_1 = \frac{1}{2}T_{10}h_1^2 + (R_0 - T_{20}h_2)h_{12} \tag{8}$$

$$\frac{1}{2}h_q \le h_p \le \frac{1}{2}h_2 \tag{9}$$

It is convenient to introduce moments of the temperature profile (1) in reference to the temperature $T_b$, since this can be taken directly from observational data once $h_2$ is selected. The definition of these moments is formally similar to (3) and (4). Thus,

$$S_0 = \int_{-h_2}^{0} (T - T_b)dz \tag{10}$$

$$S_1 = \int_{-h_2}^{0} (T - T_b)zdz \tag{11}$$

For a given location and a particular time, we find the parameters that determine the model-profile by least-square fitting its moments with respect to $T_b$ ($S_0$ and $S_1$) to the corresponding values computed using observational data. $dT_b/dt = 0$ is one of the basic assumptions of this profile. That means there is a level below which seasonal variation does not penetrate. These are taken from the observational data set compiled by Levitus (1982). The Levitus-data set provides monthly-averaged global temperature fields on a horizontal $1° \times 1°$ grid with 19 vertical levels extending from the ocean surface to a depth of 1000 m. The least-square fitting method is applied with $h_2 = 1000$ m. The procedure results in values of $h_1$, $T_1$ and $T_0$ for the monthly-mean model-profiles.

The moments with respect to $T_0$ can then be obtained from the following relations,

$$R_0 = S_0 + T_{10}h_2 \tag{12}$$

$$R_1 = S_1 + \frac{1}{2}T_{10}h_2^2 \tag{13}$$

According to the Kraus-Turner (1967) concepts, the upper ocean dynamics are governed in the one-dimensional fra-

mework, without advection and salt effects and no solar flux penetration into the ocean, by the equations

$$\frac{\partial R_0}{\partial t} = F_q \tag{14}$$

$$\frac{\partial R_1}{\partial t} = F_p \tag{15}$$

where $F_q$ is the heat flux into the ocean column, and $F_p$ is the time rate of change of turbulent kinetic energy, which provides the work necessary to change the potential energy of the column.

Using the model-profile, the Kraus-Turner relations (14) and (15) can be written as

$$\frac{F_q}{\rho C_p} = H_q\dot{T}_{10} + (T_{10} - T_{12})\dot{h}_1 \tag{16}$$

$$\frac{F_p}{\alpha\rho g} = H_pF_q + (T_{10} - T_{12})H_1\dot{h}_1 \tag{17}$$

where

$$T_{12} = \frac{F_q(H_1 + H_p) - F_p}{H_qH_1}$$

$$H_q = h_1 + \frac{1}{T_{10}}(T_{10} - T_{12})h_{12} \tag{18}$$

$$H_p = \frac{1}{2}h_1 + \frac{(H_q - h_1)H_1}{h_1} \tag{19}$$

with

$$H_pH_1 = \frac{1}{2}h_1^2 + \left(1 - \frac{T_{12} - T_{20}}{T_{10} - T_{12}}\right)h_1h_{12} \tag{20}$$

where the dots refer to time derivatives.

The first terms on the right-hand side of (16) and (17) represent the mixing of buoyant water down into the ocean column. The second terms in these equations have a more complex form, because changes below the mixed layer are not only induced by entrainment, but also by heat transfer across the mixed laye base. The potential energy balance (17) comprises the work required to distribute the heat from the surface over the system, and that performed by the entrainment process. According to the self-similarity assumption, changes in the mixed-layer temperature require changes in the thermocline profile.

The prognostic equations for the profile parameters ($T_{10}$, $h_1$, and $h_{12}$) are now obtained from (16) and (17),

$$\dot{T}_{10} = \frac{F_q(H_1 + H_p) - F_p}{H_qH_1} \tag{21}$$

$$\dot{h}_{10} = \frac{F_p - H_pF_q}{(T_{10} - T_{12})H_1} \tag{22}$$

and the diagnostic relation (2). These equations can be integrated in time if the values of $F_q$ and $F_p$ in terms of the states of the ocean and the atmosphere are available

through appropriate parameterizations, and the temperatures $T_{20}$ are known. The K-M model is based on prognostic equations (21) and (22), and the diagnostic relation (2).

*Parameterization of forcing functions*

Appropriate parameterizations for the forcing functions $F_q$ and $F_p$ are the main concern of ocean mixed-layer theories. In the K-M model, $F_q$ is approximated by the heat flux through the ocean surface, that is

$$F_q = SR - LR - SH - LH \qquad (23)$$

where $SR$ and $LR$ are solar and long-wave radiative fluxes, respectively, $SH$ is sensible heat flux, and $LH$ is latent heat flux. There are several parameterizations for $F_p$ that are generally satisfactory in the summer season, when there is a pronounced temperature gradient beneath the mixed-layer base. (Denman and Miyake, 1973; Gill and Turner, 1976). There are several competing proposals for mechanisms that prevent unrealistically large entrainment rates during winter. Several methods for reduction of the potential energy in the ocean column have been proposed in terms of dissipation (Gill and Turner, 1976). We now discuss the manner in which the K-M model addresses these issues.

Differentiating (6) with respect to time, yields

$$F_p = \alpha g \left[ \frac{1}{C_p} h_p F_q + \rho R_0 \dot{h}_p \right] \qquad (24)$$

where $g$ is gravity, $c_p$ is the heat capacity of sea water per unit mass ($4000$ J K$^{-1}$ kg$^{-1}$), $\rho$ is density of sea water ($1000$ kg m$^{-3}$) and $\alpha$ is the coefficient of thermal expansion for sea water ($\alpha = 10^{-4}$ K$^{-1}$).

The first term on the right-hand side of (24) represents the work necessary to distribute the buoyancy supplied at the surface over the ocean column for a fixed centre of gravity. The second term describes the work necessary to displace the centre of gravity of the column, while keeping the buoyancy content fixed. This displacement is essentially a consequence of entrainment processes at the mixed-layer base. According to Kraus and Turner (1967) $F_p$ work needed to displace the centre of gravity is provided by the shear generated turbulent kinetic energy. This component can be parameterized in terms of the atmospheric frictional velocity $u^*$.

Therefore,

$$\alpha g \rho R_0 \dot{h}_p = c \rho_a u_*^3 \qquad (25)$$

where $\rho_a$ is the density of air and $c$ is a nondimensional constant.

Inserting (25) into (24) gives

$$F_p = c \rho_a u_*^3 + \frac{\alpha g}{C_p} h_p F_q \qquad (26)$$

The second term in (26) provides for simulation of the observed reduction of the potential energy during the win-

ter season, when $F_q$ is negative. Previous parameterizations have relied on dissipation effects to accomplish this reduction.

A test of the parameterization (26) has been performed by Karaca and Müller (1991) using weather ship data for five different locations in the North Atlantic Ocean. They found that the optimal value for the nondimensional parameter $c$ is unity. This factor $c$ has been taken order 1 by several previous investigators (Kato and Philips, 1969; Denman and Miyake, 1973; Niiler and Kraus, 1977; Oberhuber, 1988; Bleck *et al.*, 1989). The test with weather ship data shows that the $F_p$-parameterization given by (26) successfully reproduces observed rates of change of potential energy in the ocean column and avoids unrealistically deep mixed layers during the winter season.

The K-M model, therefore, consists of the prognostic equations (21) and (22), the diagnostic relation (2), and the parameterizations (23) and (26). Note that the system is not closed, since the number of unknowns exceeds the number of equations. Since we are interested in intraseasonal time scales, however, we do not expect variations in the deep ocean. Consequently, we will use observational data to determine $T_0$ and $T_b$, and will treat them both as time-independent. Chart 1 is a schematic of the procedure used in the K-M model integrations.

*Ocean effective depth*

As stated in the Introduction to this paper, the upper ocean is characterized by a much larger heat capacity than the atmosphere. A first approach to represent oceanic effects in the coupled atmosphere-ocean system considers the ocean as a heat reservoir consisting of a layer with constant temperature. The layer depth is determined so that the heat storage of the idealized ocean matches estimates from obser-
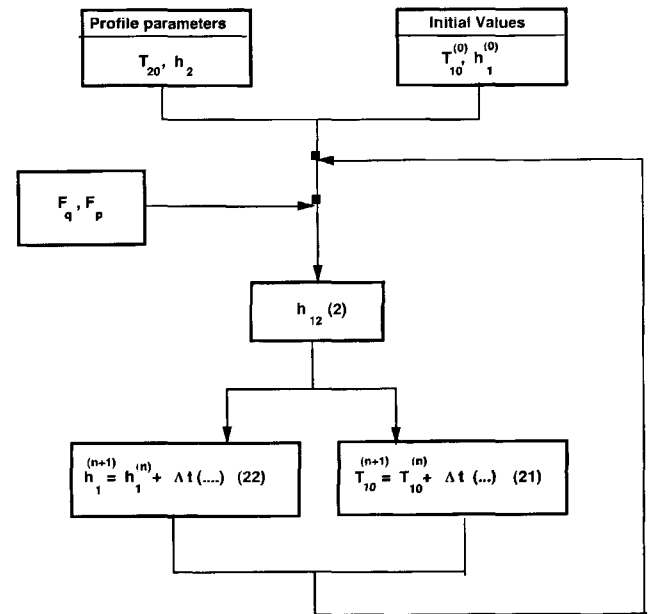


Chart 1

*Schematic representation of one-dimensional K-M model integrations.*

18

vational data. This depth is called "effective depth" (Meehl, 1984). Manabe and Stouffer (1980) derived an estimate of the effective depth using the temperature data compiled by Levitus and Oort (1977). They obtained annual means on latitudinal circles and used the global average of those means, 68 m, as the effective depth in a simple mixed-layer ocean at all locations and seasons in studies on the climatic impact of doubling $CO_2$. Van den Dool and Horel (1984) computed effective depths for the Pacific Ocean from energy balance considerations. Their values range from 25 to 50 m for the subtropical and mid-latitude Pacific.

Meehl (1984) pointed out that the mixed-layer depth is not a good approximation of the effective depth because the heat storage beneath the mixed layer is not negligibly small. A more precise effective depth, therefore, should be somewhat deeper than that of the mixed layer. These considerations are of relevance to estimates of SST based on simulated heat storage. Meehl (1984) developed a technique to compute effective depths that vary in time and space and could be used in simple ocean models suitable for coupling to AGCMs. The method used by Meehl (1984) involves two contributions to the heat storage. The first contribution – from the mixed-layer – is calculated using a depth estimated from observational data and temperature equal to the SST. The second contribution – from the seasonal thermocline – which is taken as proportional to the temperature and depth at which little or no seasonal change takes place. Meehl (1984) derived the annual cycle of zonal-mean heat storage for the Northern Hemisphere oceans in the mixed layer, and in both the mixed layer and seasonal thermocline.

The values of heat storage obtained by considering the mixed layer and thermocline show much better agreement with those obtained using observational data by Oort and Vonder Haar (1976) than their counterparts computed considering the mixed layer only. However, there are discrepancies between the results from Oort and Vonder Haar (1976) and Meehl (1984), especially at locations where advective effects are expected to be important, such as the equatorial oceans.

Using the K-M model permits a more natural calculation of heat storage in the upper ocean than Meehl's (1984) technique. This is because the model-profile (1) represents more closely the observed vertical structure of the buoyancy profile of the upper ocean than that assumed by Meehl (1984). In particular, the term we called the thermal depth in (5) is formally the effective depth if $h_2$ is taken as the depth below which seasonal variations in heat storage are negligibly small. Rewriting (5) for $h_q$ yields

$$h_p = h_1 + \frac{1}{T_{10}}(T_{10} - T_{20})h_{12} \qquad (27)$$

The second term on the right-hand side of (27) represents the contribution of the seasonal thermocline to the value of the effective depth and asymptotic temperature of the profile. Based on (27), the mixed-layer temperature and depth, and the temperature at $z = -h_2$ are the only variables required to compute the effective depth.

## The temperature structure in the upper Pacific Ocean

We focus now on the Pacific Ocean between 50° S and 50° N. Application of the least-square fitting procedure results in the values of $h_1$, $T_1$ and $T_0$ for the monthly-mean model-profiles. The corresponding values of $T_0$ and those of $T_b$ (the temperature at 1000 m depth in the Levitus-data set), have small temporal variations at specific locations. In addition, $T_b - T_0$ has small variations both in space and time. Consequently, $T_b$ and $T_0$ will be taken as constant from now on. Furthermore, we will take $T_b - T_0 = 0.1$ K.

Our results for mixed-layer temperatures and depths corresponding to February and August are shown in Figures 1 and 2, respectively. These months are chosen to illustrate winter-summer contrast in the ocean. The resolution in these figures is 4° latitude by 5° longitude, which corresponds to the standard low-resolution version of the UCLA-AGCM to be used later in this paper. Figures 1 and 2 show a pronounced seasonal signal in mid-latitudes with warm and shallow mixed layers in the summer hemisphere, and cool and deep mixed layers in the winter hemisphere, and almost no seasonal variability around the equator.

Figure 3 shows the difference between effective and mixed-layer depths for February and August. Note that seasonal variations are larger outside than in the tropics. Values are smaller than 50 m in most of the tropical Pacific. Stronger extratropical seasonal variations are in the
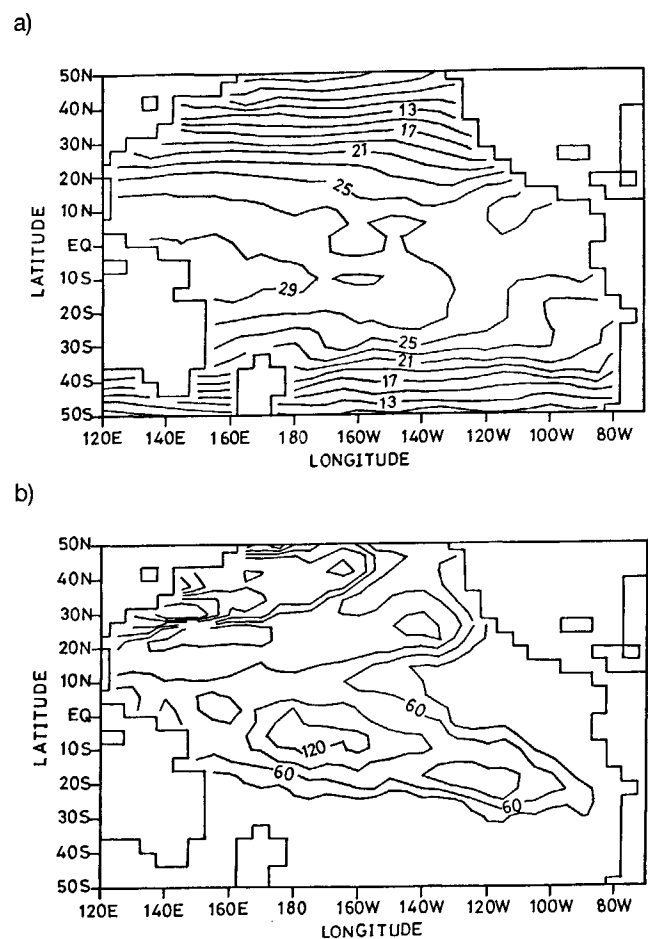
a)



b)



Figure 1

*a) Mixed-layer temperatures and b) Mixed-layer depths in the Pacific for February. Contour interval for a) 2 °C and b) 30 m.*
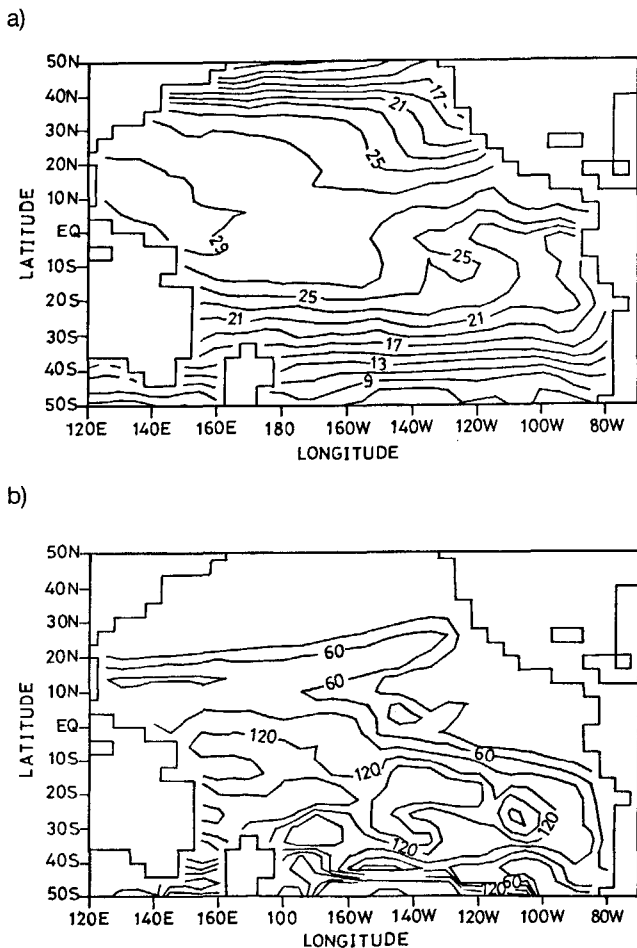
a)



b)



Figure 2

*a) Mixed-layer temperatures and b) Mixed-layer depths in the Pacific for August. Contour interval for a) 2 °C and b) 30 m.*

a)



b)



Figure 3

*Differences between effective and mixed-layer depths in the Pacific Ocean. a) February, b) August. Contour interval 10 m.*

North Pacific, with larger values in August and smaller values in February. Figure 3 clearly shows that the heat storage in the thermocline is not negligible compared to that in the mixed layer.

Since we know the profile parameters ($T_{10}$, $h_1$ and $T_{20}$) by the least-square fitting method, the zeroth moment ($R_0$) can be computed by using (7) for each month. We can approximate the local time derivative of the zeroth moment using a forward scheme in the following way;

$$\frac{\partial R_0}{\partial t} \approx \frac{R_0^{n+1} - R_0^n}{\Delta t} \qquad (28)$$

where the superscript denotes time step (month). The right hand side of (28) is shown in Figure 4 for January and July. A comparison between Figure 4 with that corresponding to heat flux at the ocean surface compiled from observational data by Esbensen and Kushnir (1981) and Oberhuber (1988) shows similarities in both pattern and magnitude, except in the equatorial regions where advective effects are expected to be important. Therefore, a good approximation to (14) in the mid-latitude Pacific Ocean is
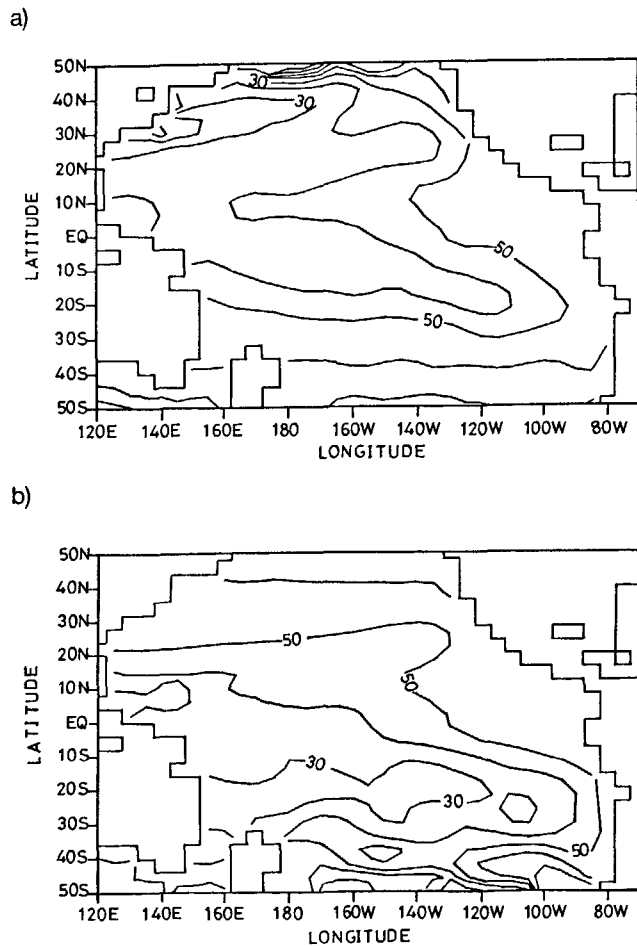
$$\frac{\partial R_0}{\partial t} = F_q \qquad (29)$$

## Seasonal evaluation of surface momentum fluxes from the UCLA-AGCM

### Methodology

In the previous Section, we show that the local time derivative of the zeroth order moment of the temperature profile is approximately equal to the surface heat flux outside the equatorial belt and away from boundary currents for the Pacific Ocean. With this understanding, we use the K-M model in the North Pacific from 22° N to 50° N, and from 130° E to 100° W; and in the South Pacific from 50° S to 22° S, and 130° E to 70° W. The model is forced with the surface heat fluxes produced by the UCLA-AGCM in a simulation with prescribed time-varying SST field in the boundary conditions. The SSTs used in the AGCM simulation are taken as the mixed-layer temperatures for the model-profile used in the K-M model. $T_1$ and $F_q$, therefore, are given. To find the mixed-layer depth ($h_1$), rate of turbulent kinetic energy ($F_p$), and mixing energy ($cu_*^3$) with the K-M model we have to specify $T_b$ and $T_0$.

Oort and Vonder Haar (1976) show that most heat stored in the ocean is in the upper 275 m. In our analysis, we chose $h_2 = 300$ m based on availability of temperature data at this level in the Levitus data set. In principle, the temperature $T_b$ should correspond to that at 300 m deep. Following this procedure, however, can result in spots where tem-
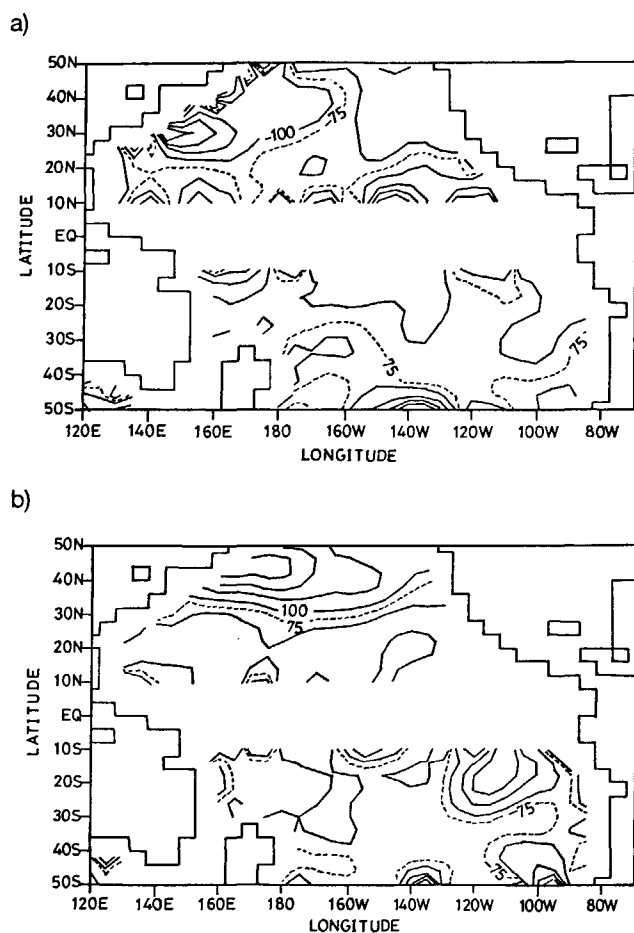
a)



b)



Figure 4

*Local time derivative of the zeroth moment. a) January, b) July. Contour interval 50 W/m².*



Chart 2

*Schematic representation of the methodology of inverse calculation mixing energy.*

peratures at 300 m depth are warmer than those taken for the mixed layer as described above. This is partly due to differences between the climatological SSTs used as boundary condition for the UCLA-AGCM (Alexander and Mobley, 1976) and those in the Levitus data set. Therefore, we construct a $T_b$ field consistent with the restriction that $T_b$ never exceeds $T_1$, but with a pattern similarity with that provided by observational data for the temperature at 300 m depth.

In the North Pacific, most climatological SSTs prescribed in the UCLA AGCM boundary conditions are minimum in March. A few of these minima can be seen in February and April. To find $T_b$, we substract 2 °C from the minimum SST-field north of 30° N, and 3 °C from the minimum SST-field south of 30° N at each grid point. In this way, the condition for the vertical stability is satisfied at all times. The field $T_b$ obtained with this procedure has a similar pattern to the annual mean temperature at 300 m depth in the Levitus data set. The asymptotic temperature, $(T_0)$, is obtained by subtracting 0.1 °C from the $T_b$ field. Therefore, $T_{20}$ is assumed 0.1 °C in the entire domain throughout the year.

To integrate the equations of the K-M model, initial values for the mixed-layer depth have to be prescribed. Karaca and Müller (1991) point out that observational data do not show clear indications of gradual retreat in the mixed-layer
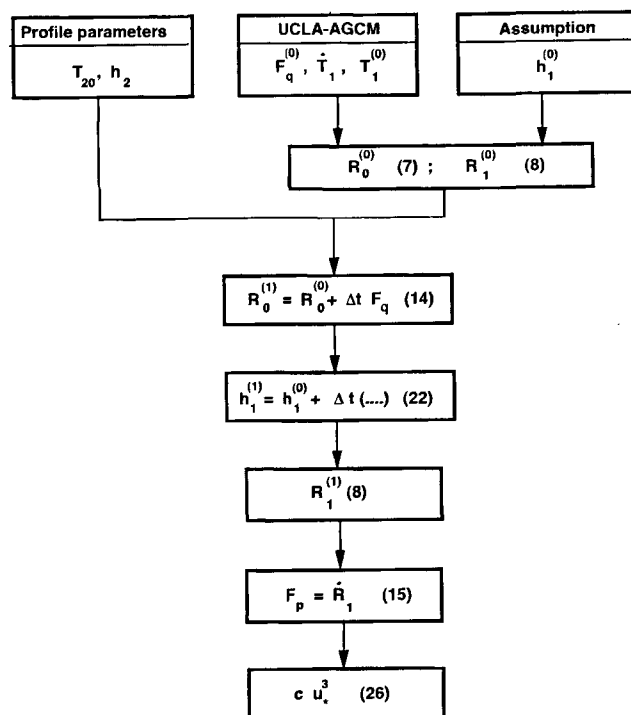
during spring. Early in spring, mixed-layer depths jump from large values to almost zero. Therefore, for locations in the Northern Hemisphere we start the integration in March, and set the initial value of the mixed-layer depth to zero in the entire domain. Similarly, for locations in the Southern Hemisphere, mixed-layer depths are set to zero at the start of the integration in September.

The calculation of the mixed-layer depths and mixing energy is carried out in the following way (*see* Chart 2). Knowledge of the surface heat flux $(F_q)$ allows for a straightforward time-marching for the zeroth moment of the temperature profile by using (3). Inserting $R_0$, $T_{10}$ and $T_{10}$ into (21) and (22), allows calculation of $h_1$ and $h_1$. The first moment of the temperature profile, $(R_1)$, can be calculated from (8) since both mixed-layer depth and temperature are known. Therefore, the time rate of change of the turbulent kinetic energy, $(F_p)$, can be obtained from (15). Since $F_q$, $F_p$, $R_0$ and $R_1$ are already known, the mixing energy $(cu_*^3)$ can be easily computed from (26).

*Results for the North Pacific*

The mixed-layer depths for the North Pacific obtained with the method described above are shown in Figure 5 for January and July. Mixed layers are generally deep in the former season and shallow in the latter season. In both January and July, deeper mixed layers are found in the northern part of the domain.

The seasonal cycle of zonally averaged mixed layer depths is shown in Figure 6a. Winter months show deeper mixed layers than summer months; largest values for the former months are near 45° N. In magnitude and pattern the mixed-layer depths are very similiar to those compiled

from Robinson's data (1976) as shown by Meehl (1984) for the North Pacific (*see* his Fig. 4). The maximum mixed-layer depth obtained with the K-M model is around 120 m in February. The analysis performed by Meehl (1984) shows maximum values of about 110 m around 45° N also in February.

The seasonal cycle of zonally-averaged effective depths obtained with the K-M model is shown in Figure 6*b*. Comparison of the values in Figure 6 with those obtained by Meehl (1984, *see* his Fig. 15) reveals that the former are about 10 m-20 m deeper than the latter. There are similarities, however, in the evolutions of those fields. The larger differences occur in summer, when the effective depths obtained with the K-M model are shallower than those obtained by Meehl (1984).

The seasonal cycle of zonally-averaged $cu_*^3$ is represented in Figure 7*a*, which shows largest values in October around 40° N-45° N, and a secondary maximum in February. Similar maxima for the same months are also found by Elsebery and Garwood (1980) for weather ships P (50° N, 145° W) and V (34° N, 160° W). The magnitude of $u_*^3$ decays from mid-spring to a minimum value in summer, and strenght tens again in early autumn. The October maximum is associated with the passage of storms. Our analysis with the K-M model, therefore, shows that intense mixing is needed to start the deepening of the mixed layer in the autumn season (Fig. 7).

The most recent estimates of $u_*$ are obtained by Oberhuber (1988) using the COADS data set. There is pattern similarity between our results for $cu_*^3$ and those of Oberhuber for $u_*$ (1988, *see* his Fig. 16.1-16.12).

Figure 7*b* shows the seasonal zonally-averaged $u_*^3$ obtained from the UCLA-AGCM. The largest values produced by the AGCM are found in the winter months. The lack of pattern similarity between Figures 7*a* and 7*b* implies that the differences between values of $cu_*^3$ produced by the K-M model and those of $cu_*^3$ produced by the AGCM cannot be simply explained by a constant factor $c$. If $c$ is taken of order unity, then the AGCM values are a great deal smaller than the K-M model values and the corresponding observational estimates. Contour plots of $cu_*^3$ produced by the K-M model are shown in Figure 8 for January and July, respectively. The corresponding values of $cu_*^3$ produced by the AGCM are shown in Figure 9.

Figure 10 shows the seasonal evolution of the zonally-averaged values of $T_1$ corresponding to the SST prescribed in the AGCM, surface heat flux simulated with the AGCM, and zeroth-moment of the model-profile from the K-M model. It is apparent that variations in the heat content of the upper Pacific Ocean at mid-latitudes lag about one month behind those in SST. For example, the minimum and maximum of $T_1$ in March and September are followed by minimum and maximum of heat stored in April and October, respectively. Together with Figure 5, these results show that deep mixed layers are generally associated with cooler SSTs, while shallower mixed layers are generally associated with warmer SSTs in mid-latitudes. Figure 10*c* shows that deep and shallow mixed layers are associated with large and small heat content in the mid-Pacific, respectively. Since deeper mixed layers are found north of
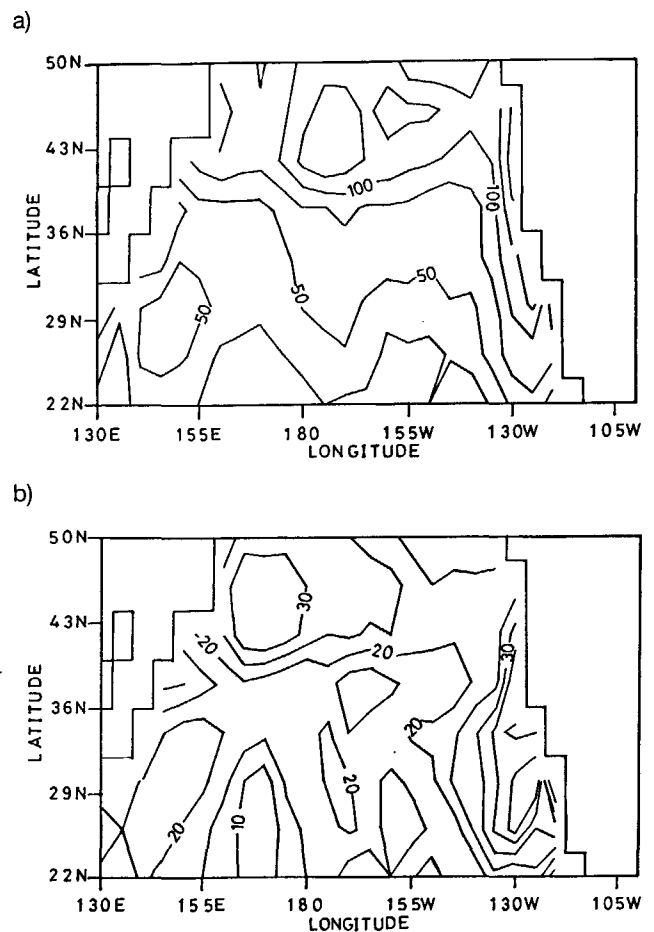
a)



b)



Figure 5

*Mixed-layer depths in the North Pacific Ocean. a) January, contour interval 25 m, b) July, contour interval 5 m.*

40° N, the upper Pacific ocean stores more heat in the extratropics than in the subtropics.

We repeated the analysis described above by using the surface heat fluxes produced in a simulation with the AGCM in which the SSTs correspond to those observed during the period March 1983 through February 1984. This is an interesting period since it corresponds to the decaying phase of the strongest El Niño (ENSO) Southern Oscillation event on record.

The differences between climatological and observed SSTs used in the AGCM, and those obtained in simulated surface heat fluxes are shown in Figure 11. Figure 12 shows the corresponding differences in $h_1$, $R_0$ and $cu_*^3$. Negative anomalies in $T_1$ (*i.e.* in SST) approximately correspond to positive differences in surface heat fluxes, mixed-layer depths, and mixing energy. It appears that increased heat fluxes into the ocean are distributed vertically to establish deep mixed layers by stronger wind mixing. In general, the heat content of the upper ocean obtained with the K-M model for the AGCM simulation with observed SSTs is larger than that for the climatological SSTs. Overall cooling is dominant in most places and at most times except south of the 36° N and north of 45° N from September 1993 to March 1994. The zonally-averaged anomalous atmospheric heat flux is also larger at the same places and
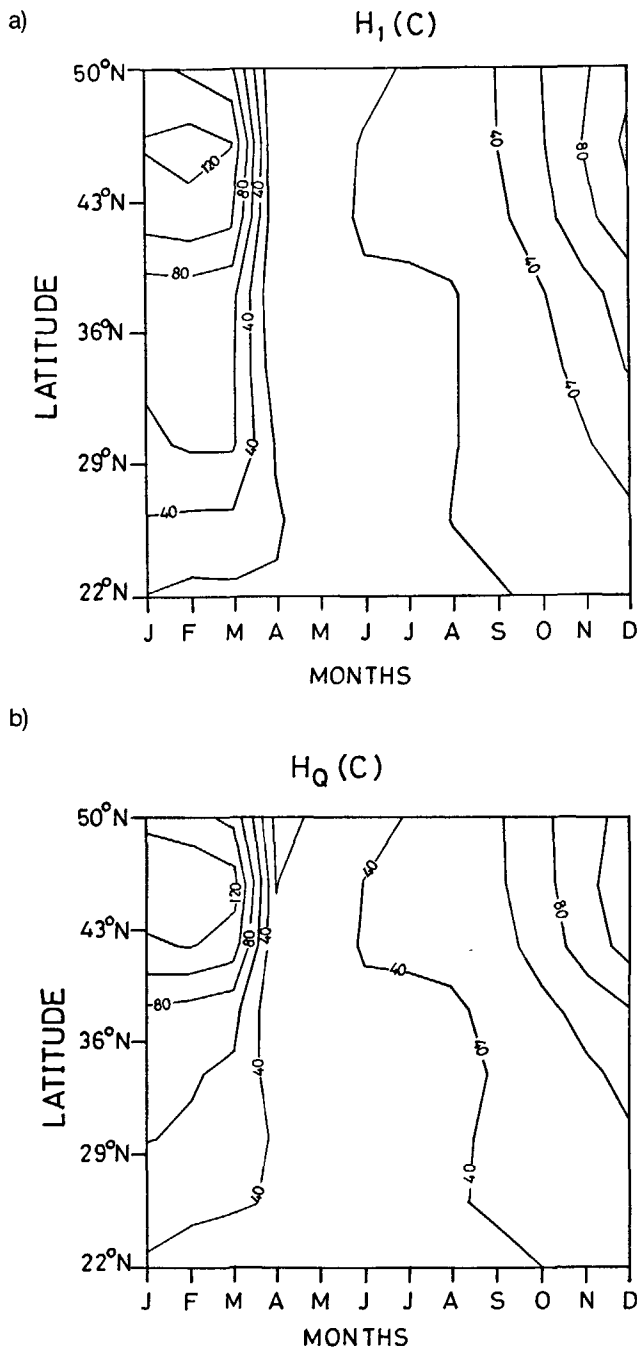
a)



b)



Figure 6

*a) Zonally-averaged climatological mixed-layer depths; b) Zonally averaged climatological effective depths for the North Pacific Ocean. In both pictures, contour interval 20 m.*

a)



b)



Figure 7

*a) Zonally-averaged climatological ($cu_*^3$) produced by the mixed-layer model. Unit is $m^3/s^3$. b) Zonally-averaged climatological ($u_*^3$) produced by AGCM. Units are 0.1 $m^3/s^3$.*

times. This means the ocean lost heat during most of that period. Figure 12 clearly confirms this with deeper mixed layers negative heat contents and mixing energies throughout this period and in most of the domain.

## SUMMARY AND CONCLUSIONS

A model for the upper ocean is presented in the framework of Kraus and Turner (1967) concepts. The model, which we have called the K-M model, has two distinctive features:
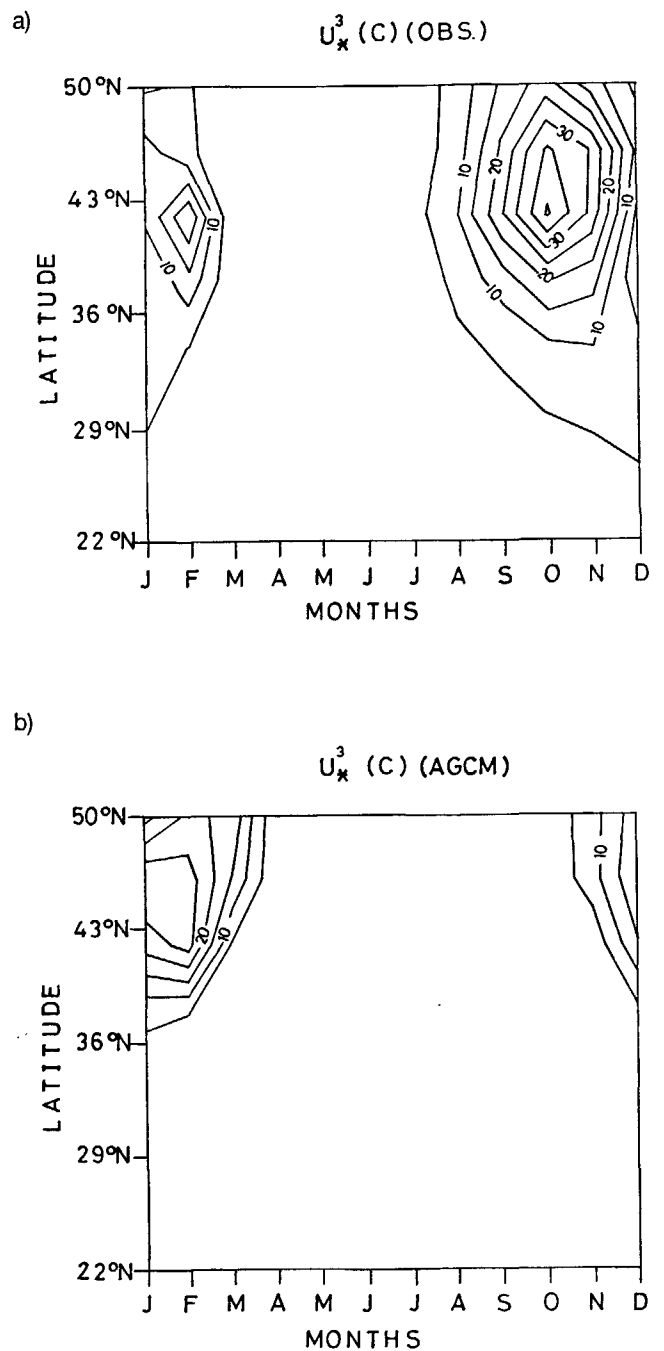
a) it is based on a self-similar temperature profile called the model-profile; and

b) it uses special parameterizations of forcing functions in terms of surface heat fluxes and wind stress. The model-profile presents the advantages of simplicity and a convincing physical picture. A merit of the approach to modelling the upper ocean used in the K-M model is that no vertical discretization is required.

An important feature is the parameterization for $F_p$, the rate of the turbulent kinetic energy. The parameterization, which is based on the entrainment effects of turbulent kinetic energy, is shown to be consistent with observed rates of
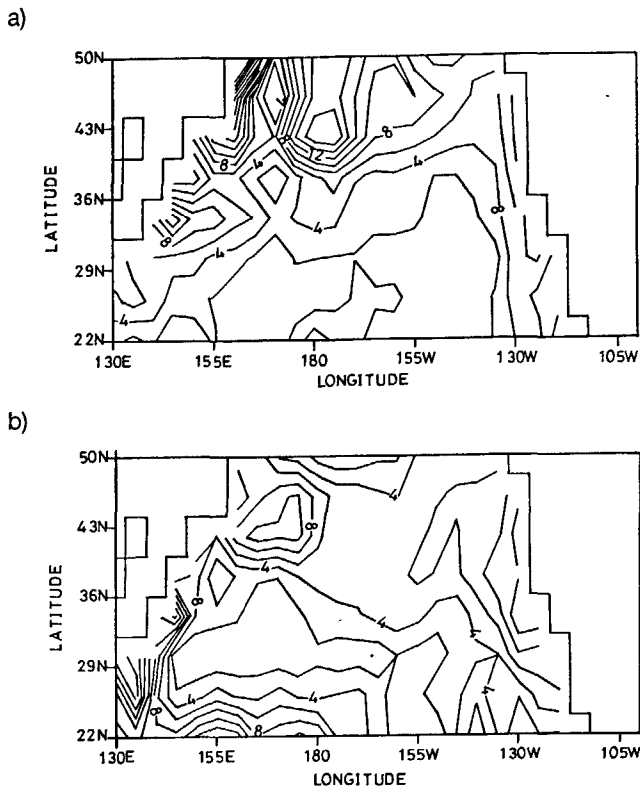
a)



b)



a)



Figure 8

*Climatological cu³ₓ produced by the mixed-layer model: a) January, unit is m³/s³; b) July, 0.2 m³/s³.*

a)



b)



b)



c)
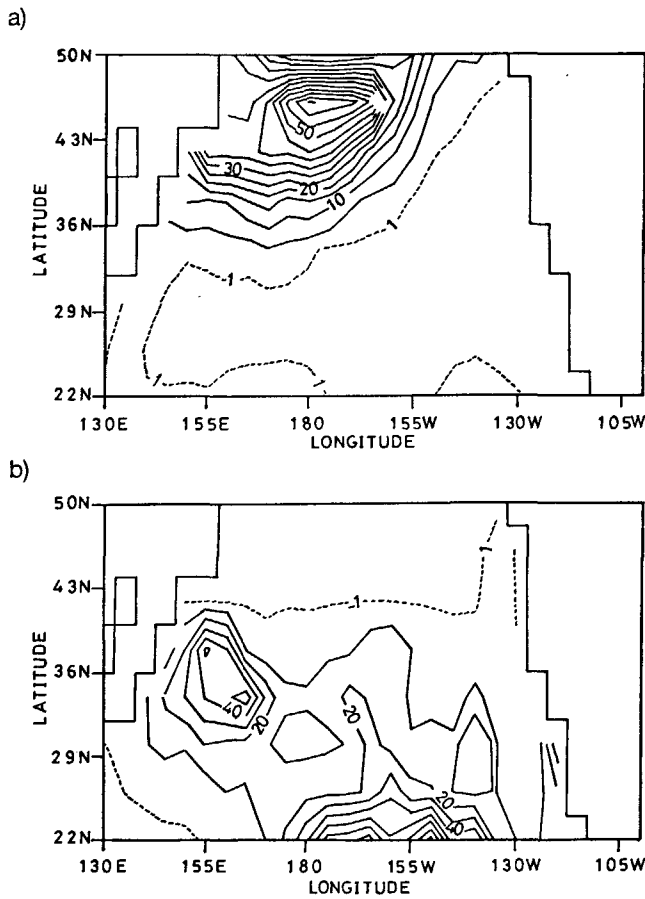


Figure 9

*Climatological cu³ₓ produced by AGCM: a) January, unit is 0.1 m³/s³; b) July, 0.02 m³/s³.*
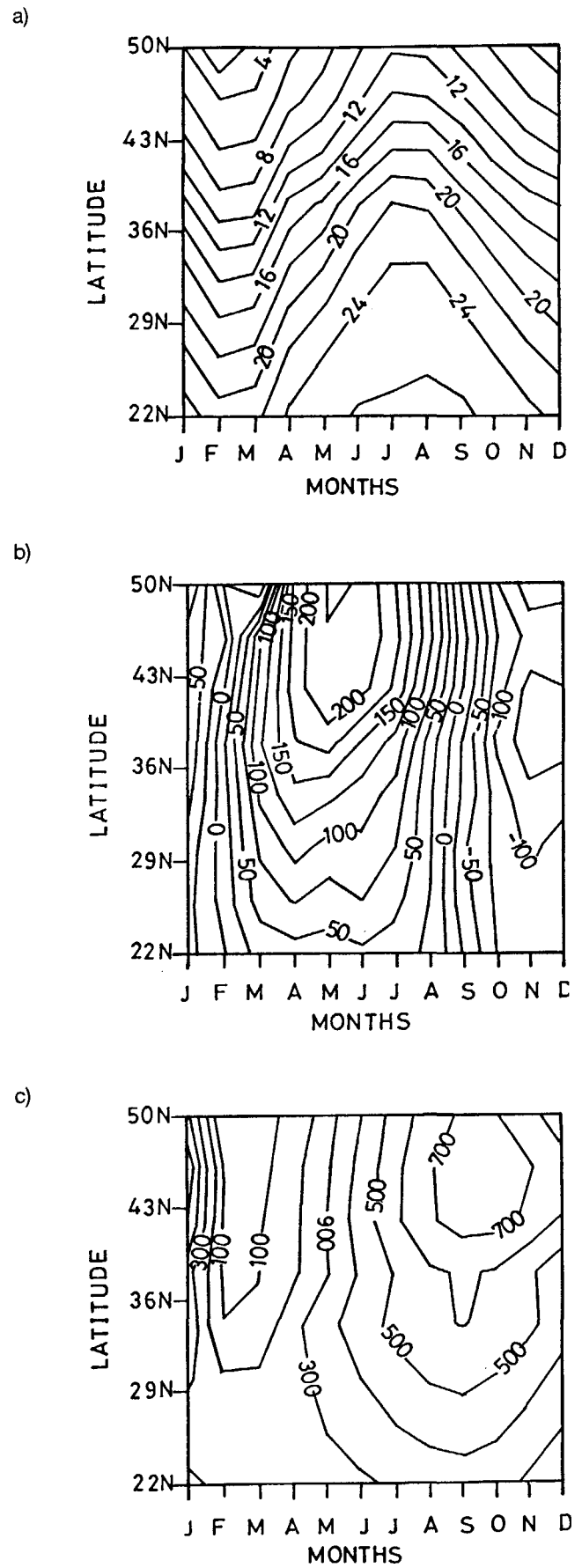
Figure 10

*Zonally-averaged climatological values of: a) mixed-layer temperature; b) surface heat flux; and c) zeroth moment for the North Pacific Ocean.*
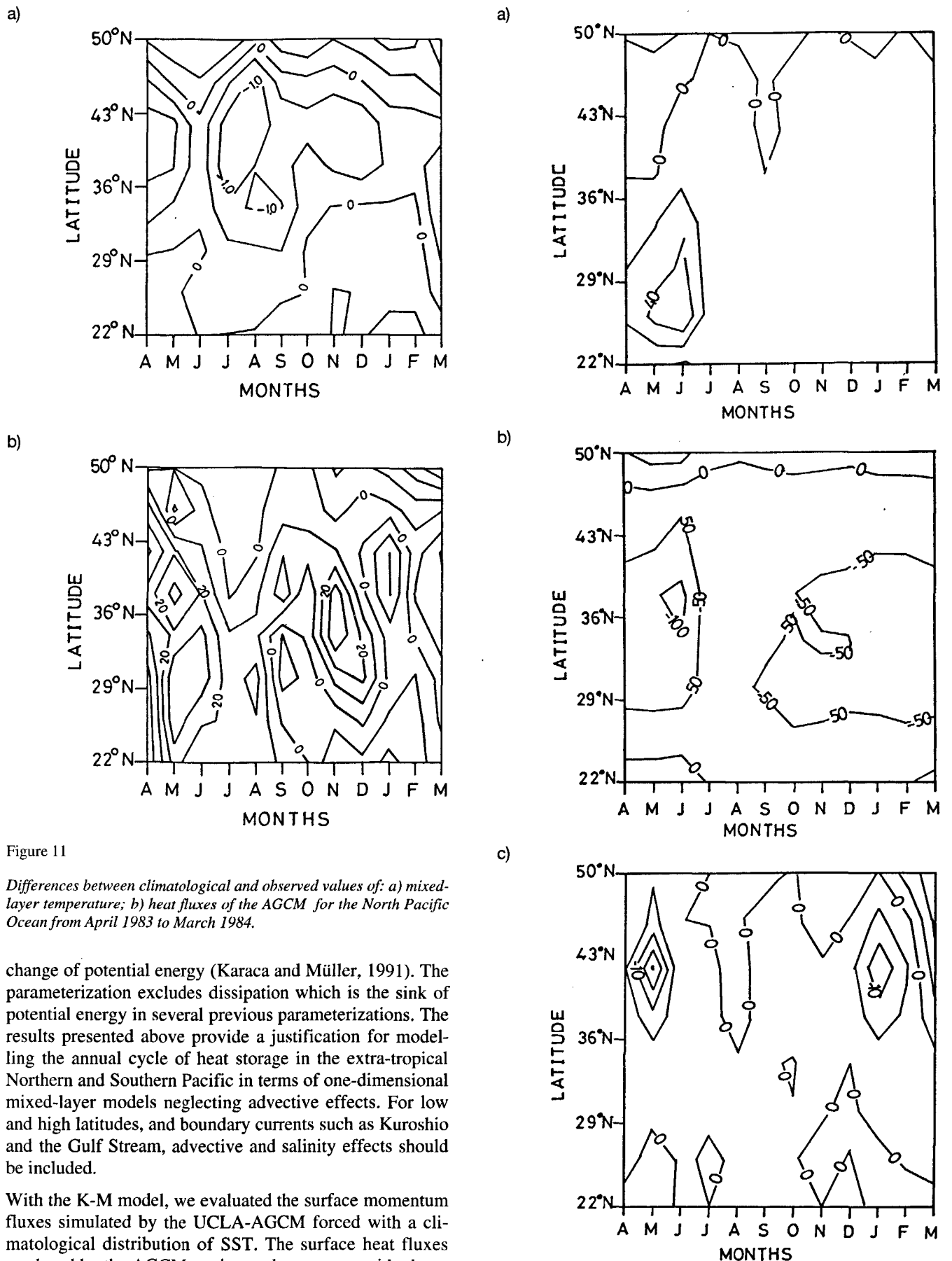
a)



b)



Figure 11

*Differences between climatological and observed values of: a) mixed-layer temperature; b) heat fluxes of the AGCM for the North Pacific Ocean from April 1983 to March 1984.*

change of potential energy (Karaca and Müller, 1991). The parameterization excludes dissipation which is the sink of potential energy in several previous parameterizations. The results presented above provide a justification for modelling the annual cycle of heat storage in the extra-tropical Northern and Southern Pacific in terms of one-dimensional mixed-layer models neglecting advective effects. For low and high latitudes, and boundary currents such as Kuroshio and the Gulf Stream, advective and salinity effects should be included.

With the K-M model, we evaluated the surface momentum fluxes simulated by the UCLA-AGCM forced with a climatological distribution of SST. The surface heat fluxes produced by the AGCM are in good agreement with observational data. This agreement is partly due to the use of prescribed SSTs as the lower boundary condition in the AGCM simulations. We show that the mixing energy at the sea surface produced by the UCLA-AGCM is weaker

a)



b)



c)



Figure 12

*Differences between climatological and observed values of: a) mixed-layer depth; b) zeroth moment; and c) mixing energy $(cu_*^3)$ for the North Pacific Ocean from April 1983 to March 1984.*

than that obtained with the K-M model. The magnitudes of momentum fluxes produced by UCLA-AGCM are too small, because in general, AGCMs use unrealistically high friction to time their models numerically. An investigation of patterns of momentum fluxes are also questionable. The K-M model produced high values of mixing energy near the western boundary which are needed for the model but those of UCLA-AGCM do not have (Fig. 8 and 9).

We also used the K-M model to obtain the heat content of the upper ocean for the extra-tropical Pacific using the fluxes produced during an AGCM simulation using climatological SSTs for the period October 1982-September 1983. In these simulations the mixed layer depth and (the third power of) the frictional velocity are calculated for given surface heat flux and mixed-layer temperature. Pattern-wise, the calculated frictional velocities coincide satisfactorily with COADS data compiled by Oberhuber (1988). In conclusion, the momentum fluxes at the ocean surface diagnosed by the model forced with the heat fluxes and SSTs of the UCLA-AGCM show substantial differences with those produced by the UCLA-AGCM. In the Northern Pacific the mixed-layer and effective depth agree well with observations published by Meehl (1984).

The climatology analysis indicates that the maximum heat storage at a given location occurs from several weeks to two months after the SST maximum. The region of maximum heat storage is found poleward of the maximum SST in both hemispheres.

In the analysis in which observed SSTs are used, the atmosphere was characterized by anomalously strong winds in the North Pacific. This led, in general, to deeper mixed layers and cooler SSTs. The heat storage in the upper ocean, on the other hand, generally exceeded the climatological condition in the North Pacific. We conclude from these results that the upper ocean in the mid-latitudes stores heat most effectively at moderate mixed layer depths, which occur for moderate temperatures. High mixed layer temperatures are generally associated with shallow mixed layers, while deep mixed layers are associated with low mixed layer temperatures. The changes in the heat content of the upper ocean do not imply changes in the structure of the buoyancy field. The mixing energy is mainly responsible for establishing the buoyancy structure of the upper ocean. Therefore, after the El Niño of 1982-83 the upper ocean structure is significantly different from climatology. These differences are associated with others in the atmospheric circulation.

## Acknowledgements

## REFERENCES

Alexander R.C., L. Mobley (1976). Monthly average sea-surface temperatures and ice pack limits on a 1° global grid. *Mont. Weath. Rev.* 104, 143-148.

Bleck R., H.P. Hanson, D. Hu, E.B. Krauss (1989). Mixed layer-thermocline interaction in a three-dimensional isopycnic coordinate model. *Jour. Phys. Oceanogr.* 19, 1417-1439.

Denman K.L., M. Miyake (1973). Upper layer modification at ocean station Papa; observations and simulations. *Jour. Phys. Oceanogr.* 3, 185-196.

Esbensen S., Y. Kushnir (1981). The heat budget of the global ocean: An atlas based on estimates from surface marine observations. Climate Research Institute, Report no. 29, Oregon State University. Corvallis, OR 97331, USA.

Gill A.E., J. Turner (1976). A comparison of seasonal thermocline models with observation. *Deep Sea Res.* 23, 391-401.

Karaca M., D. Müller (1989). Simulation of sea-surface temperatures with surface heat fluxes from an atmospheric circulation model. *Tellus* 41A, 32-47.

Karaca M., D. Müller (1991). Mixed-Layer Dynamics and Buoyancy Transports. *Tellus* 43A, 350-365.

Kraus E.B., J.Turner (1967). A one-dimensional model of the seasonal thermocline. *Tellus* 19, 98-105.

Lemke P. (1987). A coupled one-dimensional sea-ice model. *Jour. Geophys. Res.* 72, 13164-13172.

Lemke P., T. Manley (1984). The seasonal variation of the mixed-layer and the pycnocline under polar sea ice. *Jour. Geophys. Res.* 69, 6494-6504.

Levitus S. (1982). Climatological atlas of the world ocean. NOAA, Rockville, MD.

Manabe S., R.J. Stouffer (1980). Sensitivity of a global climate model to an increase of $CO_2$ concentration in the atmosphere. *Jour. Geophys. Res.* 85, 5529-5544.

Meehl G.A. (1984). A calculation of ocean heat storage and effective ocean surface layer depths for the Northern Hemisphere. *Jour. Phys. Oceanogr.* 14, 1747-1761.

Niiler P.P. (1975). Deepening of the wind-mixed layer. *Jour. Mar. Res.* 33, 405-422.

Niiler P.P., E.B. Kraus (1977). One-dimensional models of the upper ocean, in Modeling and Prediction of the Upper Layers of the Ocean, E.B. Kraus, Ed. p. 143-172, Pergamon Press, New York.

Oberhuber J. (1988). An atlas based on the 'COADS' data set: The budgets of the heat, buoyancy and turbulent kinetic energy at the surface of the global ocean. Report no. 15, MPI für Meteorologie, Hamburg, FRG.

Oort A.H., T.H. Vonder Haar (1976). On the observed annual cycle in the ocean-atmosphere heat balance over the Northern Hemisphere. *Jour. Phys. Oceanogr.* 6, 781-800.

Pollard D., M.L. Batteen, Y.J. Han (1983). Development of a simple upper-ocean and sea-ice model. *Jour. Phys. Oceanogr.* 13, 754-768.

Robinson M.K. (1976). Atlas of North Pacific Ocean monthly mean temperatures and mean salinities of the surface layer. Naval Oceanographic Office, Washington, D. C., 173 p.

Van den Dool H.M., J.D. Horel (1984). An attempt to estimate the thermal resistance of the upper ocean to climatic change. *Jour. Atmos. Sci.* 41, 1601-1612.